Effects of high-energy electrons provided by dielectric barrier discharge on chemical reactions in plasma-assisted burner flame

誘電体バリア放電から供給される高エネルギー電子が
プラズマ支援バーナー火炎中の化学反応にもたらす効果

Kazunori Zaima and Koichi Sasaki
財満和典，佐々木浩一

Division of Quantum Science and Engineering, Graduate School of Engineering, Hokkaido University
Kita 13, Nishi 8, Kita-ku, Sapporo 060-8628, Japan
北海道大学大学院 工学院 量子理工学専攻 〒060-8628 札幌市北区北13条西8丁目

We examined the spatial distributions of density of atomic oxygen and rotational temperature of OH($A^2\Sigma^+(v'=0)$) in premixed flame assisted by dielectric barrier discharge. The density of atomic oxygen changed synchronously with the current pulse in the preheating region between the unburned and reaction zones. OH($A^2\Sigma^+(v'=0)$) with a lower rotational temperature, which was suspected to be in close relationship with improved combustion reactions, was appeared synchronously with the current pulses in the preheating region. It is suggested that the activation of combustion reactions is triggered by additional atomic oxygen produced in the preheating region.

1. Introduction

Plasma-assisted combustion is a novel technique to reduce the consumption of fossil fuels by achieving ultralean combustion with the help of high-energy electron in nonequilibrium plasmas. However, the microscopic role of high-energy electrons has not been understood well. In this work, we focused on the role of high-energy electrons in combustion chemistry. We introduced high-energy electrons into a premixed burner flame by superposing a dielectric barrier discharge (DBD).

2. Experimental setup

We employed a premixed burner with CH_4/O_2/Ar mixture. The flow rates of CH_4, O_2, and Ar were adjusted to 0.38, 1.0, and 5.6 slm, respectively, using mass flow controllers. The length of the flame was approximately 85 mm. The side of the slender flame was partly covered with a quartz tube. The distance between the bottom side of the quartz tube and the top of the burner nozzle was 13 mm, and the length of the quartz tube was 65 mm. An aluminum electrode was attached on the outside of the quartz tube. The distance between the bottom side of the electrode and the top of the burner nozzle was 25 mm, and the axial length of the electrode was 10 mm. A high-voltage power supply with a rectangular waveform was connected to the aluminum electrode, while the burner nozzle worked as the ground electrode. We thus obtained asymmetric DBD inside the quartz tube.

We adopted conventional optical emission spectroscopy using an imaging spectrograph for measuring the optical emission spectra of Ar and the $A^2\Sigma^+(v'=0) - X^2\Pi(v''=0)$ transition of OH. We carried out data analyses for evaluating the spatiotemporal variations of the optical emission intensity and the rotational temperature of OH($A^2\Sigma^+(v'=0)$).

One-dimensional two-photon absorption laser-induced fluorescence (TALIF) was applied for measuring the density of atomic oxygen. Pulsed OPO laser beam at a wavelength of 225.58 nm was focused into the DBD-assisted flame. The distance between the laser beam and the burner nozzle was 3 mm. The intensity of the laser beam was uniform in the observation area, so that the LIF intensity gave us the one-dimensional (radial) distribution of the relative density of atomic oxygen. The oscillation of the OPO laser was synchronized with the high voltage waveform of DBD, and we obtained the temporal variation of the atomic oxygen density by changing the delay time between the applied high voltage and the laser oscillation.

3. Results

The density of atomic oxygen had the following radial distribution. The atomic oxygen density in the unburned zone was negligible, and it increased steeply at around r=1.0 mm. The maximum density was observed in the reaction zone at r=1.5 mm. We observed radial decrease in the atomic oxygen density in the burned side of the reaction zone, and the density at r=5.0 mm was almost negligible.

The overall radial distribution of the atomic oxygen density was hardly affected by the superposition of DBD, except for the decrease in

the density in the outside region (r=3-5 mm). However, by taking a closer look, we noticed the change in the atomic oxygen density in the preheating region between the unburned and reaction zones. Figure 1(a) shows the temporal variation of the atomic oxygen density at the radial positions of r=1.0, 1.5 and 2.0 mm. The vertical axis is normalized by the atomic oxygen density in the absence of DBD. As shown in the figure, the densities at the radial positions of 1.5 and 2.0 mm were roughly unaffected by DBD at all the discharge phases. On the other hand, the density at a radial position of 1.0 mm was dependent on the discharge phase, and the oscillations of $[O_{ON}]/[O_{OFF}]$ were observed at around the timings of the current pulses.

Figure 1(b) shows the temporal variation of the rotational temperature of $OH(A^2\Sigma^+(v'=0))$ at a radial position of 1.0-1.3 mm. The dashed horizontal line in the figure represents the rotational temperature in the absence of DBD. As shown in the figure, the decreases in the rotational temperature beyond the error bar were observed at 0, 0.1 and 0.6 ms.

4. Discussion

The radial positions of r=1.0, 1.5 and 2.0 mm correspond to the preheating region, the reaction zone, and the burned side of the reaction zone, respectively. The unchanged density of atomic oxygen in the reaction zone indicates the fact that atomic oxygen is produced via combustion reactions dominantly even in the DBD-assisted flame. However, the combustion reactions are surely improved by DBD, since the decrease in the atomic oxygen density in the outside region represents the increase in the burning velocity.

The origin of the improved combustion is observable in the preheating region. The synchronization between the bulge in $[O_{ON}]/[O_{OFF}]$ and the current pulse, which was observed at r=1.0 mm, indicates that a remarkable amount of additional atomic oxygen is produced by electron impact dissociation of molecular oxygen. The bugle was followed by the rapid decrease in $[O_{ON}]/[O_{OFF}]$, which is probably caused by the overconsumption of atomic oxygen via combustion reactions. The oscillation of $[O_{ON}]/[O_{OFF}]$ suggests a kind of competition between the production of additional atomic oxygen and its overconsumption, but it is important to note here that the oscillation of $[O_{ON}]/[O_{OFF}]$ is observed only in the presence of the current pulses. The atomic oxygen in the preheating region has the response to high-energy electrons.

In a previous paper, we have reported that the rotational temperature of $OH(A^2\Sigma^+(v'=0))$ also has the response (the decrease) to high-energy electrons [1]. In addition, we have suggested that $OH(A^2\Sigma^+(v'=0))$ with cold rotational temperature is produced by $CHO+O \rightarrow OH(A^2\Sigma^+)+CO$. The measurement of the rotational temperature was not resolved spatially in the previous work, but in this work, we confirmed the decrease in the rotational temperature of $OH(A^2\Sigma^+(v'=0))$ in the preheating zone as shown in Fig. 1(b). Therefore, the production of additional atomic oxygen in the preheating region is consistent with the decrease in the rotational temperature of $OH(A^2\Sigma^+(v'=0))$. The present work suggests that the additional production of atomic oxygen in the preheating region triggers the enhanced combustion in the DBD-assisted flame.

Reference

[1] K. Zaima and K. Sasaki: Jpn. J. Appl. Phys. **53** (2014) 110309.

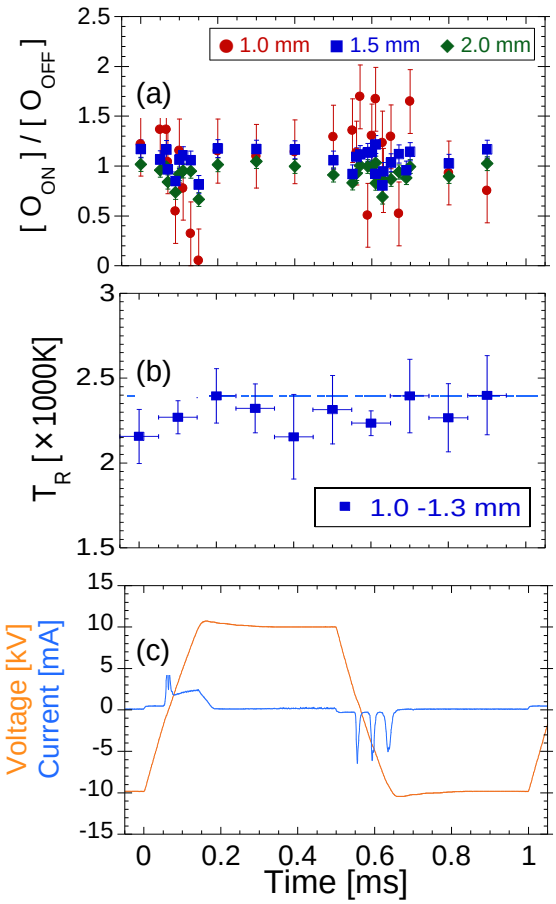

Fig. 1. Temporal variations of (a) the density of atomic oxygen, (b) the rotational temperature of $OH(A^2\Sigma^+(v'=0))$ at a radial position of 1.0-1.3 mm. (c) represents the waveforms of the discharge voltage and current.